**ORIGINAL**

CrossMark

# A non-contact method for the determination of fibre direction of European beech wood (*Fagus sylvatica* L.)

**Thomas Ehrhart**[1,2] · **René Steiger**[2] · **Andrea Frangi**[1]

## Abstract

This paper introduces a non-contact method for the identification, quantification, and documentation of fibre direction of European beech wood (*Fagus sylvatica* L.). The developed approach is based on an automated visual analysis of the spindle pattern formed by the medullary rays, also termed wood rays. Each spindle is identified by means of image analysis technique, its position and orientation is determined, and the fibre direction of discretised elements is calculated. The individual process steps necessary to obtain an estimate of the fibre direction of a board are explained using the examples of five different failure types. In all examples, the estimated fields of fibre direction are congruent with the actual fibre direction determined by means of (1) the orientation of all present shrinkage cracks, which are established indicators for the fibre direction in wood, and (2) the fracture pattern after tensile testing. Employing the presented approach could open up new possibilities for the characterisation of European beech and other hardwood species with multi-row medullary rays in several fields of application, in particular regarding stress grading.

## 1 Introduction

The fibre direction has an influence on most physical properties of wood. Amongst others, the electrical and thermal conductivity, swelling and shrinking, and the strength and stiffness properties strongly depend on the considered orientation relative to the fibre direction. In wood segments free of knots, bark inclusions, or any other local defect, i.e. in so-called clear wood, wood can be described approximately as a cylindrically anisotropic material using the three main directions longitudinal (*L*), tangential (*T*), and radial (*R*) (Fig. 1) and the properties mentioned above can be related to these directions. Considering the *T* and *R* directions together as orientation *perpendicular to the grain* is in many cases well-appropriate, sufficient, and therefore a frequently applied simplification.

However, in reality, a plurality of characteristics has an impact on the general and local fibre direction in wood.

Spiral growth, strong conical shape, and curvature of trunks cause general slope of grain, whereas local fibre deviations occur primarily in the vicinity of knots. Both types of slope of grain result in locally changed material properties compared to clear wood. Thus, methods allowing for the determination of fibre direction are of highest interest in several fields of application of wood, in particular, however, regarding stress grading. In view of the above, several methods, systems, and products available on the market, aiming for a fast, accurate, and precise determination of fibre direction, have been developed in the past 50 years based on different physical principles.

The dielectric properties of wood are strongly anisotropic, i.e. the magnitude of permittivity is highest in the *L*-, and lowest in the *T*-direction. Based on the analysis of the elliptical polarisation of originally linear polarised electromagnetic waves, methods for the assessment of fibre orientation by using microwave scanning have been developed (Norimoto and Yamada 1972; Baradit et al. 2006; Denzler and Weidenhiller 2015).

Besides microwave scanning, measurement of the electrical field strength constitutes another radiographic approach for the indication of fibre direction (Norton et al. 1974; Cramer and McDonald 1989; Steele et al. 1991). When applying a sinusoidal electrical field to a wooden board, the abovementioned dielectric properties lead to a phase shift,

✉ Thomas Ehrhart
ehrhart@ibk.baug.ethz.ch

1 Institute of Structural Engineering, ETH Zürich, Stefano-Franscini-Platz 5, 8093 Zurich, Switzerland

2 Structural Engineering Research Laboratory, Empa-Materials Science and Technology, Ueberlandstrasse 129, 8600 Dubendorf, Switzerland
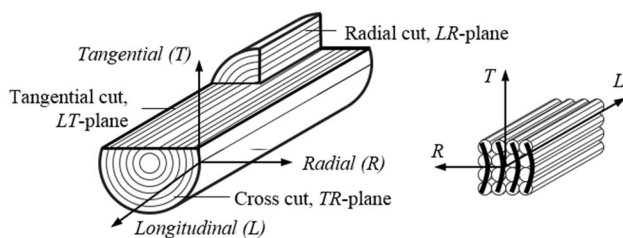
**Fig. 1** Cylindrical anisotropy of wood, and the three main directions longitudinal (L), tangential (T), and radial (R) on (global) trunk level (left) and on (local) fibre level (right)

which itself is correlated with the fibre orientation. One major advantage of radiographic approaches is the possibility to not only evaluate the wood surface but the entire volume of a board. However, additional influential parameters, in particular wood density and moisture content, have to be considered and appropriate correction calculations of the generated data to account for diffraction at edges are required when using microwave scanning or electrical field strength measurement for assessing the fibre direction.

Employing the so-called tracheid effect is another possibility to determine the fibre direction (Matthews and Beech 1976; Matthews and Soest 1986; Soest 1997; Metcalfe and Dashner 2002; Nyström 2003; Simonaho et al. 2004; Sarén et al. 2006). This approach harnesses the effect that a light beam (e.g. laser light) hitting the surface of wood is conducted parallel to the fibres much stronger than perpendicular. Thus, the reflected part of the light has an elliptical form, whereby the principal axis orientates parallel to the fibre direction. This method has been widely addressed in descriptions and models of wood and its structure (Foley 2001; Lukacevic and Füssl 2014; Briggert et al. 2016) as well as for a further development of strength grading of wood (Brännström et al. 2008; Olsson et al. 2013; Viguier et al. 2015, 2017; Olsson and Oscarsson 2017). However, in contrast to radiographic approaches, this method is limited to information gained from the scanning of the wood's surface and, thus, the quality of the estimated three-dimensional field of fibre orientation decreases with increasing thickness or width of the examined specimen.

A recently proposed approach for the measurement of the fibre direction is based on the thermal conduction properties of wood (Daval et al. 2015; Belkacemi et al. 2016). Following the suggested method, the wood's surface is excited with a line of laser dots and the elliptically shaped heat conduction pattern is captured by means of an infrared camera. Similar to the method employing the tracheid effect, information regarding the fibre direction is derived from the orientation of the ellipse's principal axis. Again, the so-called thermal ellipsometry method (Krapez et al. 1996) has to be considered as a surface scanning method.

The focus of the vast majority of the abovementioned research conducted in this area was on softwood timber species. In studies carried out in Central- and Northern Europe, especially Norway spruce (*Picea abies* Karst.) was investigated; in most North American studies, Douglas fir (*Pseudotsuga menziesii* Mirb.) or Southern Pine (*Pinus taeda* L.) was focused.

Taking account of the ongoing change in climate, forest agencies in many European countries have started promoting an increased cultivation of domestic hardwood timber species. One species expected to profit from this silvicultural trend is European beech (*Fagus sylvatica* L.). Today, European beech already has a share of 60–82% of the entire hardwood resources in Austria, Germany, Slovenia, and Switzerland (Sauter and Breinig 2016; Federal Office for the Environment FOEN 2014). Due to the broad availability but also the high strength and stiffness potential of European beech wood, its use for structural purposes is expected to strongly increase in the near future, which could complement established building products made from softwoods, and broaden the application spectrum of timber at the expenses of less environmental friendly materials.

One reason frequently reported to limit the usable strength of the raw material (Frühwald 2004; Glos and Denzler 2004; Blaß et al. 2005; Ehrhart et al. 2016b), the achievable strength of finger joints (Aicher et al. 2001; Clerc and Volkmer 2017), and, consequently, the practical usage of European beech timber for structural applications is the difficulty in determining the fibre direction. Due to the small number of knots compared to most softwood species, the fibre direction plays a key role in understanding and predicting the mechanical behaviour of European beech timber.

Schlotzhauer et al. (2016) applied the abovementioned methods for the determination of fibre direction based on the electric field strength measurement, microwave scanning, and tracheid effect on European beech wood. Comparison of the measured values with visually determined splitting angles (reference) showed that the tracheid effect is hardly applicable to beech. For specimens with straight grain or little grain deviation, the electrical field strength measurement gave best results, i.e. the differences between the measured and reference angle were below 5° for more than 90% of the data. However, in specimens with moderate and strong grain deviation, the method is reported not to provide data of sufficient accuracy and, thus, further improvement would be needed.

Daval et al. (2015) applied the thermal ellipsometry to determine the fibre direction of Norway spruce (*Picea abies* Karst.), Douglas fir (*Pseudotsuga menziesii* Mirb.), and the deciduous timber species poplar (*Populus*) and oak (*Quercus petraea* Matt.). As the method turned out to be suitable also for oak wood, its ability to determine the

fibre direction of European beech wood seems to be very much worth to be investigated as well.

Standardised methods for the determination of fibre direction are the scribing method (EN 1310 1997) and the alignment of drying cracks on the flat sawn face (DIN 4074-5 2008). Following the first-mentioned method, the path of a swivel-handled scribe, pulled along a board's surface, should follow the fibres and, thus, indicate their direction. The latter method employs the effect that drying cracks in wood generally propagate parallel to the fibres. When considering the flat sawn face, the cracks are formed in the *LR*-plane. Both methods were reported not to be expedient to be applied to European beech wood (Frühwald and Schickhofer 2005).

Within a study on the tensile strength of European beech timber and its influential parameters (Ehrhart et al. 2016a, b), two observations with regard to the fibre direction were made. Firstly, the dominating failure mode was shear failure along the spindles formed by the medullary rays without crushing of individual fibres. Independent of whether the failure could be due to slope of grain around a knot, local slope of grain, dive angle, general slope of grain, or splinter failure, the fracture path was almost always prescribed by the spindle pattern formed by the medullary rays (Fig. 2a–d).

Secondly, all present drying cracks ran parallel to the spindles (Fig. 3). As already mentioned, the use of drying cracks for the assessment of fibre direction is implemented in EN 1310 (1997). Thus, analysis of the medullary ray spindle pattern can be considered as a standardised method for the determination of fibre direction, without having to rely on cracks due to shrinkage that might occur later but actually are not wanted since they lead to minor wood quality.

Ashby et al. (1985) outlined the important role of the medullary rays regarding the fracture and toughness of wood. According to Ashby et al. (1985), "*cracks in the TR orientation seek rays and propagate along them*". Thus, "*[…] rays are planes of weakness, allowing a low-energy, peeling mode of fracture*". Investigations by Frühmann et al. (2003) on the mode I fracture behaviour (opening mode) in the *TR* crack propagation plane showed that medullary rays play a dominant role, especially for European beech wood.

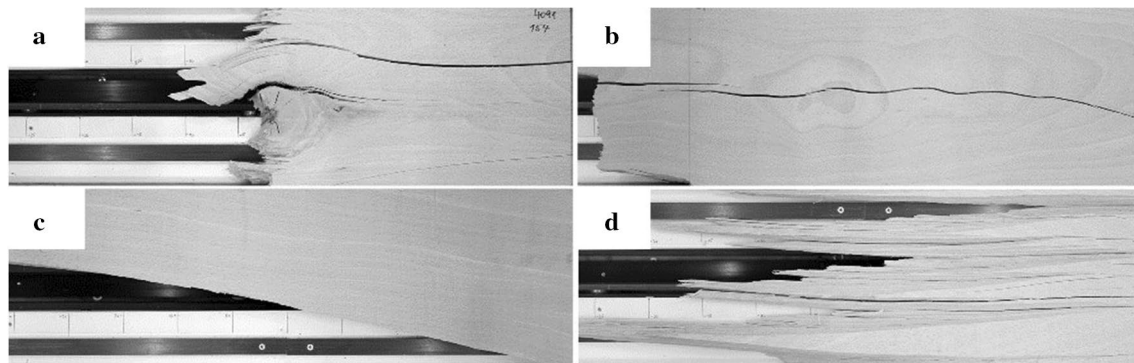Thus, a very simple model for the description of the wood anatomy and potential planes of shear failure (of



**Fig. 2** Common failure patterns observed in tensile testing of European beech wood: **a** local slope of grain around a knot, **b** local slope of grain, **c** general slope of grain, and **d** splinter failure



**Fig. 3** Drying cracks running parallel to the spindles formed by the medullary rays

European beech) is: the annual rings and the medullary rays together form corridors in which the fibres run. Due to the low shear strength of European beech wood in the *LR*-plane, the orientation of the spindles, formed by the medullary rays, is a very strong indicator for the *crucial fibre direction*. In a perfect flat sawn board, the weak planes formed by the medullary rays are parallel to the edge face and, thus, the crucial fibre direction can be identified looking at the spindle pattern on the wide face. Reversely, in a perfect quarter-sawn board, the weak *LR*-plane is parallel to the wide face and its local orientation can be identified looking at the edge face.

The spindle pattern of the species European beech is visible to the naked eye and, thus, suitable for an image analysis based approach for the estimation of fibre direction, as will be shown below. Similar to methods employing the tracheid effect or thermal ellipsometry, the proposed method is based on the scanning of the wood's surface and, thus, an assessment of the entire wood volume is not possible. However, progress of fibres in interior parts of the wood can at least be estimated.

## 2 Materials and methods

A non-contact method for the determination of fibre direction based on the analysis of the medullary rays was developed. The method will be described and discussed applying it to planed European beech timber boards with a length of 3000 mm, a cross section of $160 \times 25$ mm$^2$, and a moisture content of $8 \pm 2\%$.

In order to illustrate the principle of the method, its capabilities, but also its constraints, five boards showing different failure types in tensile tests were selected for this study, namely:

- *Type 1*: Slope of grain around a knot of a flat sawn board (Fig. 7)
- *Type 2*: Local slope of grain on the face side of a flat sawn board (Fig. 8).
- *Type 3*: Local slope of grain on the edge side of a quarter-sawn board (dive angle, Fig. 10).
- *Type 4*: General slope of grain of a flat sawn board (Fig. 11).
- *Type 5*: Splinter failure of a flat sawn board (Fig. 12).

### 2.1 Recording of the boards

To facilitate an automated analysis and processing of the images, a standardised perspective, object position, object distance, resolution, and illumination level was aimed for. Therefore, a simple device including a camera, illumination, guide rails, and a vertical slot for edge face recording was built (Fig. 4). A commercial *Nikon D7100* digital single lens reflex camera with a sensor resolution of $6000 \times 4000$ pixels (24 megapixels), and a standard lens (*Nikkor AF-S DX 18–105 mm f/3.5–5.6G IF-ED VR*) were used. The specific focal width *f* causing the least distortion of the images ($f = 24$ mm) was chosen.

All four faces of the timber boards were photographed section by section with a section length of 500 mm ($+50$ mm image overlap at both ends), resulting in 24 images for each board of 3000 mm length and an actual resolution of 100 pixels per mm$^2$. Due to the manual feeding of the apparatus and the scanning of all four faces, as only one camera was used, four runs for one single board were required, the actual speed of the process was limited to approximately 30 boards or 90 m per hour.

Regarding the used equipment there is, for sure, potential for optimisation. However, the aim of this paper is explicitly not to present a highly optimised, ready-to-run system for

**Fig. 4** Developed device for the recording of the medullary ray spindle pattern of European beech timber boards
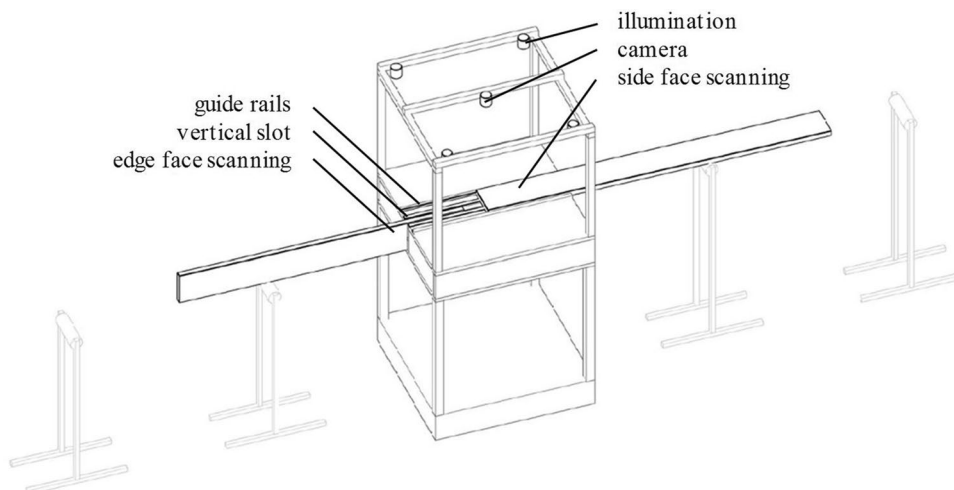
the identification and analysis of the medullary ray spindles but to point out their importance and the great potential of employing them for the determination of fibre direction in European beech wood.

## 2.2 Processing of the images

The images were processed automatically by means of batch runs using the program *Adobe Photoshop CS6*. Open source alternative programs (e.g. *GNU image manipulation program, GIMP*) with similar possibilities are available.

Due to the sensor's aspect ratio of 3:2 and the elongated shape of the area of interest ($500 \times 160$ mm$^2$), parts of the image do not contain information usable for the further process. These parts were cropped in order to reduce the file size from approximately 5.5 to 3 MB. The medullary ray spindles were isolated and identified as objects by means of image analysis technique. This leads to image information exclusively focusing on the objects of interest, the spindles, and a reduction of the file size from approximately 3 MB to 100 kB (Fig. 5).

## 2.3 Image analysis

After reducing the images to the objects of interest (spindles, black) and background (white), their content was analysed and quantified. The position and orientation of each object was automatically determined using the open source program *Image Processing and Analysis in Java, Image J*. One simple way to generate the required information is to use the calliper (or Feret-) diameter, which describes the perpendicular distance between two parallel planes touching an object's contour. The inclination of the parallels causing the largest calliper diameter was documented and used to describe the orientation of each object.

Finally, a list of information of all objects including the following parameters was compiled and used for further processing of the data:

- Area $A$ in pixels.
- Circularity $c$, calculated using Eq. (1) based on the area $A$ and perimeter $P$.
- Maximum calliper diameter in pixels, and associated orientation of the objects in degree.
- Coordinates of the objects in pixels.

$$c = 4 \cdot \pi \cdot \left( \frac{A}{P^2} \right) \tag{1}$$

## 2.4 Processing of the generated data

Based on the generated data, the field of fibre direction was estimated. Each image was discretised into elements with a size of $10 \times 10$ mm$^2$. For the analysis of the edge faces, the element size was reduced to $5 \times 5$ mm$^2$. Noise was eliminated by defining thresholds regarding object size (40–400 pixels, corresponding to 0.4–4.0 mm$^2$; the size of the spindles lies between naturally defined limits), circularity (0.01–0.30), and a maximum angle of 70°.

The coordinates of the remaining objects were used to identify the angle within one discretised element (arithmetic mean). Figure 6 shows an example of the resulting estimated field of fibre direction in numerical and vectorised form. To obtain sound and stable results, fibre direction was not estimated for segments with less than three identified objects meeting the requirements mentioned above.

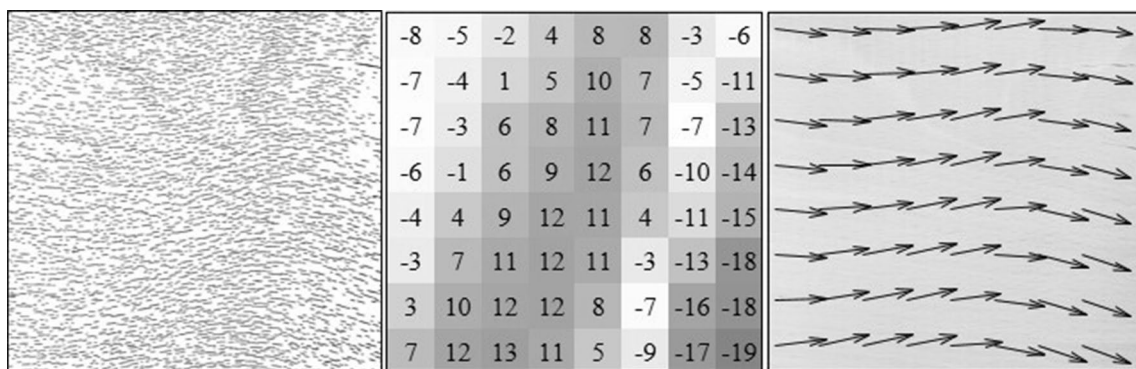**Fig. 5** Detail of an original image (left) and medullary ray spindles after processing (right)
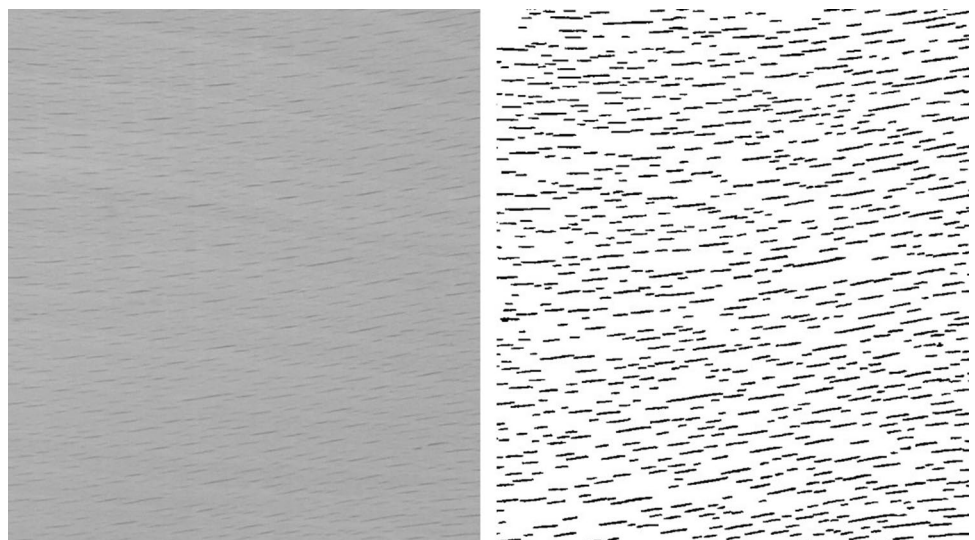
**Fig. 6** Identified medullary ray spindles and estimated field of fibre direction in numerical and vectorised form (left to right)

## 2.5 Tensile tests to determine the actual fibre direction

Tensile tests according to EN 408 (2012) were carried out. In line with previous studies (Frühwald 2004; Schlotzhauer et al. 2016), the fracture path was considered to reveal the true fibre direction and serves as a reference for the evaluation of the estimates. The cross section of the planed boards was $160 \times 25$ mm$^2$, their length 3000 mm, and the moisture content was $8 \pm 2\%$. The free test length (inner distance between the clamping jaws) was 2060 mm.

## 3 Results and discussion

The method has been applied to five boards, each of them exhibiting one of the five different failure types (type 1–5) described above. The estimated field of fibre direction was compared to the actual failure pattern resulting from the tensile tests.

### 3.1 Evaluation of the method by means of five different failure types

Figure 7 shows the estimated field of fibre direction of a board containing a knot in vectorised form, and the fracture pattern resulting from the tensile test (grain pattern type 1).

**Fig. 7** Estimated field of fibre direction and fracture pattern of a board containing a knot (grain pattern type 1)
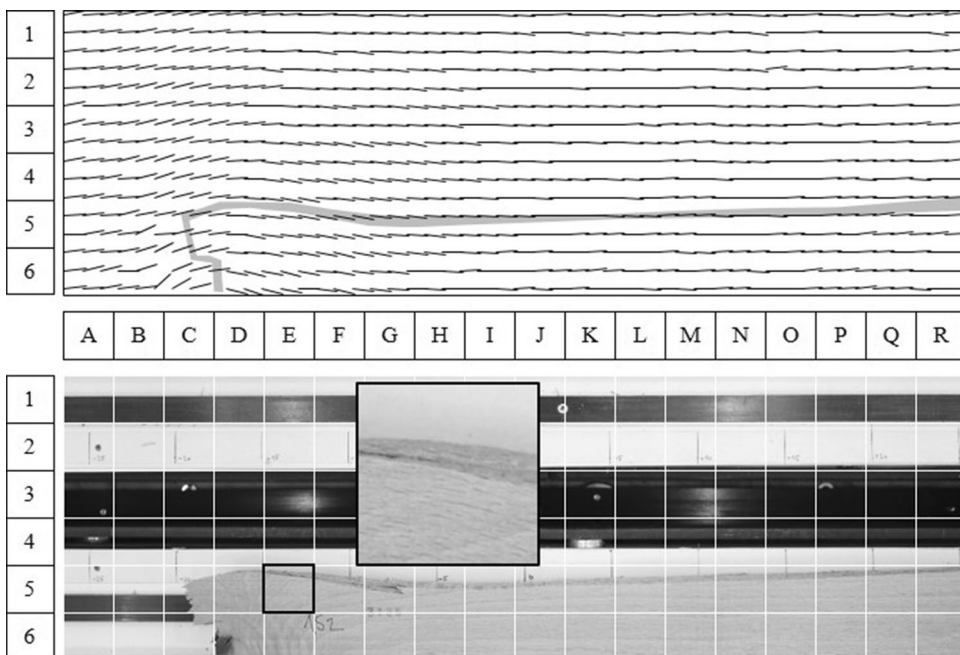
To facilitate the comparison between estimate and reference, the fracture pattern is sketched with grey colour.

On the right hand side of the image (rows H–R), a fibre angle close to zero is estimated, which agrees well with the straight fracture pattern resulting from the tensile tests. On the left hand side of the estimated field of fibre direction (columns A–G), where the knot is located, the vectors change their orientation in close correspondence to the fracture path around the knot. Furthermore, the estimate reveals that large parts (all lines of columns A–E) of the board's width are strongly affected by the knot. A closer look at the fracture path confirms that it follows the medullary ray spindles, based on which the field of fibre direction was estimated. As the fibre direction changes rapidly within a short distance around the knot, a reduction of the element size could further improve the estimate. The fracture mechanism along the medullary rays can, in agreement with Ashby et al. (1985) and Frühmann et al. (2003), be described as peeling off of the wood fibres without crushing of the fibres themselves.

However, knots constitute obvious weakening and the grain flow around the knot is expected to, at least qualitatively, look like this. Thus, and due to the much smaller number of knots in European beech timber compared to most softwood species, application and investigation of the method on boards free of knots, as described in the following, are of particular interest.

A detailed view of the estimated field of fibre direction in Fig. 8 (grain pattern type 2, top) shows that the wavelike fracture path (bottom) could be predicted well. Furthermore, the estimated fibre direction of 15°–25°

in the columns P–R is confirmed by the fracture pattern. Although this fracture path is considered to occur rather rarely, it clearly illustrates the great potential of the presented method. Again, a closer look at the fracture path confirms that it follows the medullary ray spindles perfectly.

So far, two plain sawn boards were investigated. Knots often closely pass by quarter- or rift sawn boards, without actually running through them and, thus, cause fibre deviations with an inclination to the wide face, so-called dive angle (Fig. 9). Depending on the thickness of a board, this deviation can strongly affect the entire cross section and cause a severe drop of the tensile strength.

Figure 10 shows the estimated field of fibre direction (top) and the failure pattern (grey) in the edge face of a quarter-sawn board with a high dive angle. The estimated field of fibre direction indicates that a knot ran just next to the board's upper edge as the fibres are orientated downwards at the left side and turn to an upward orientation on the right half of the image. The actual fracture pattern is equal to the estimate. Thus, the knot, which had been cut off, can be "reproduced" with the model, and its effects on the fibre direction can be correctly assessed (despite cutting it off) when evaluating the local material properties of the board.

Fibre deviation may not only occur locally. General slope of grain is often even more difficult to identify with the naked eye, as the surface pattern is very even without any obvious disruptions of the wood structure.

In Fig. 11 a plain sawn board with general slope of grain (grain pattern type 4), continuously changing from approximately 14°–10° from columns A to R, is shown. Again, the

**Fig. 8** Estimated field of fibre direction and fracture pattern of a board failed due to local slope of grain (grain pattern type 2)
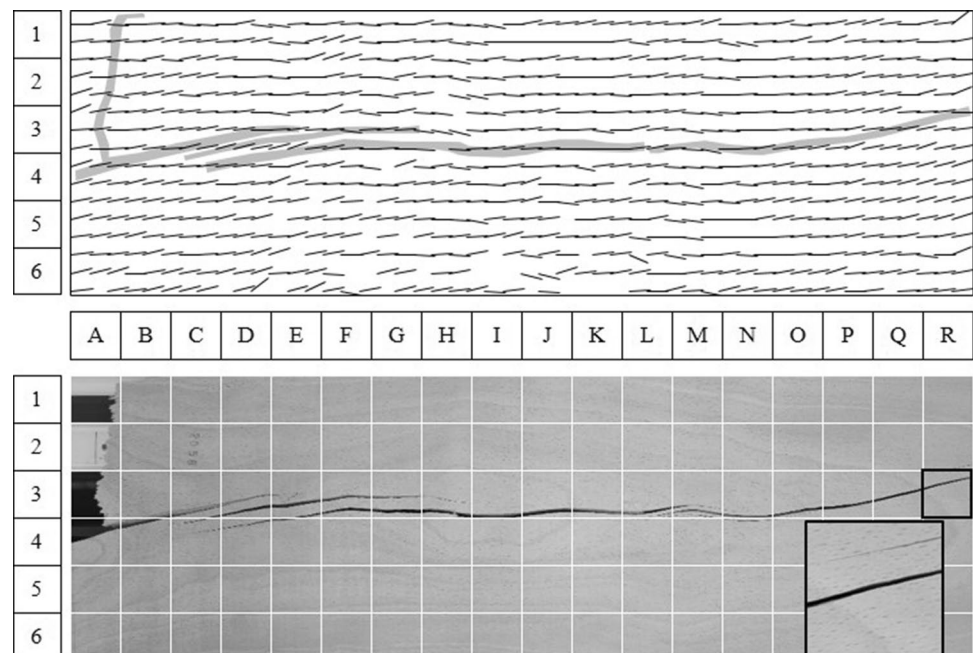
**Fig. 9** Simplified schema of a knot (black) running close to a quarter-sawn board causing a high dive angle within the area marked by the dashed lines
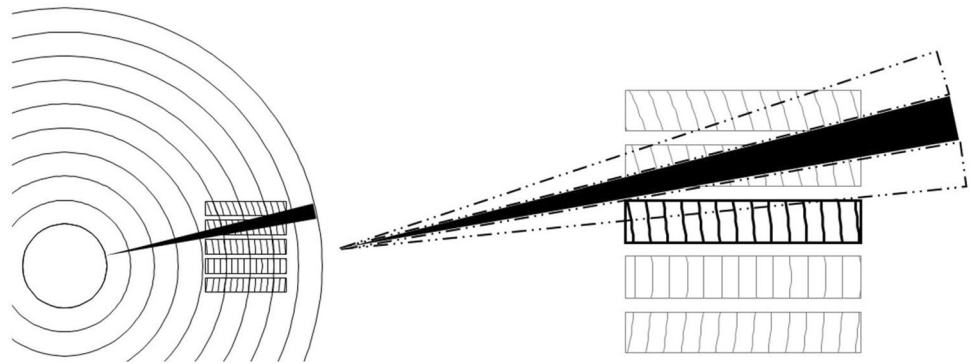


**Fig. 10** Estimated field of fibre direction and fracture pattern of a quarter-sawn board with a high dive angle, type 3
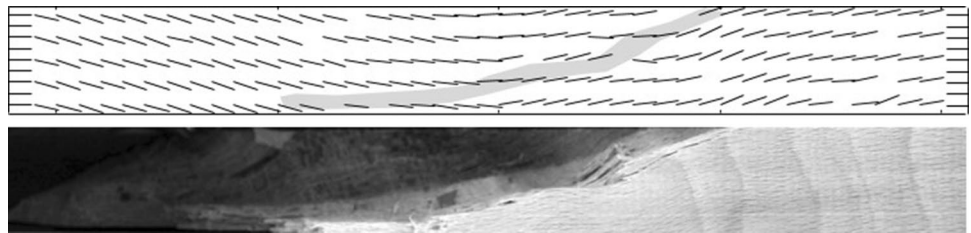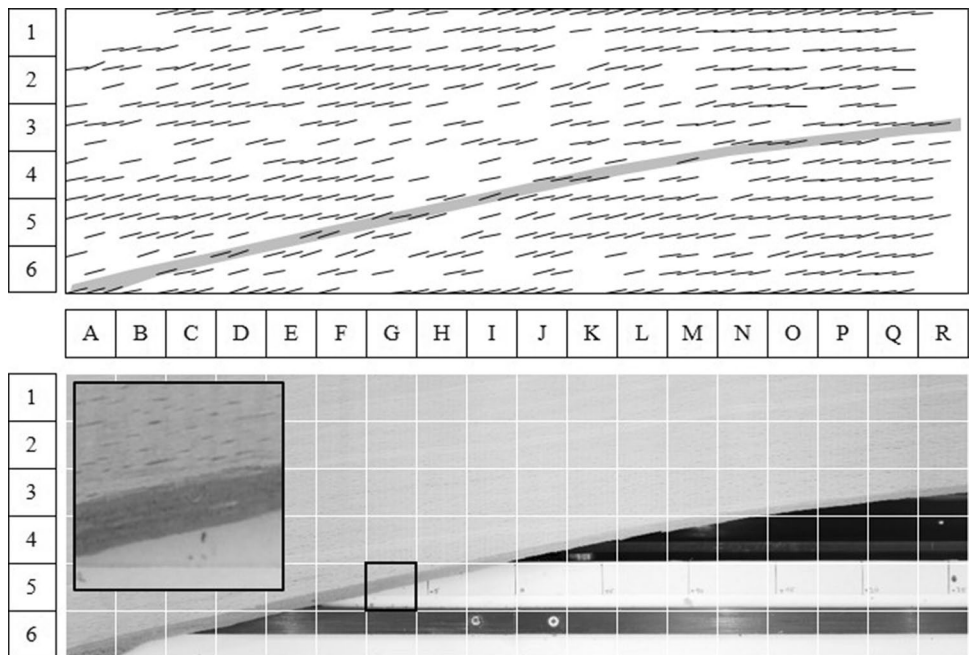


**Fig. 11** Estimated field of fibre direction and fracture pattern of a board failed due to general slope of grain, grain pattern type 4



fracture pattern is congruent with the estimated field of fibre direction.

In timber boards with straight grain, which means that the fibre direction of the entire wood volume lies below approximately 5°, regularly splinter failure occurs (grain pattern type 5, Fig. 12). This failure type is characterised by multiple shear failures along the grain and accompanied by the highest tensile strength values of between 80 and 130 MPa (Ehrhart et al. 2016a). The example in Fig. 12 shows the estimate of the fibre direction of a straight-grained board, and the associated fracture pattern after tensile testing. Both the estimate and the enlarged detail of the fracture pattern agree well with the assumption that the medullary rays constitute the weakest planes and predetermine the fracture path, which runs almost horizontally within single lines (1–6) through all columns A–R.

**Fig. 12** Estimated field of fibre direction and fracture pattern of board showing splinter failure (grain pattern type 5)
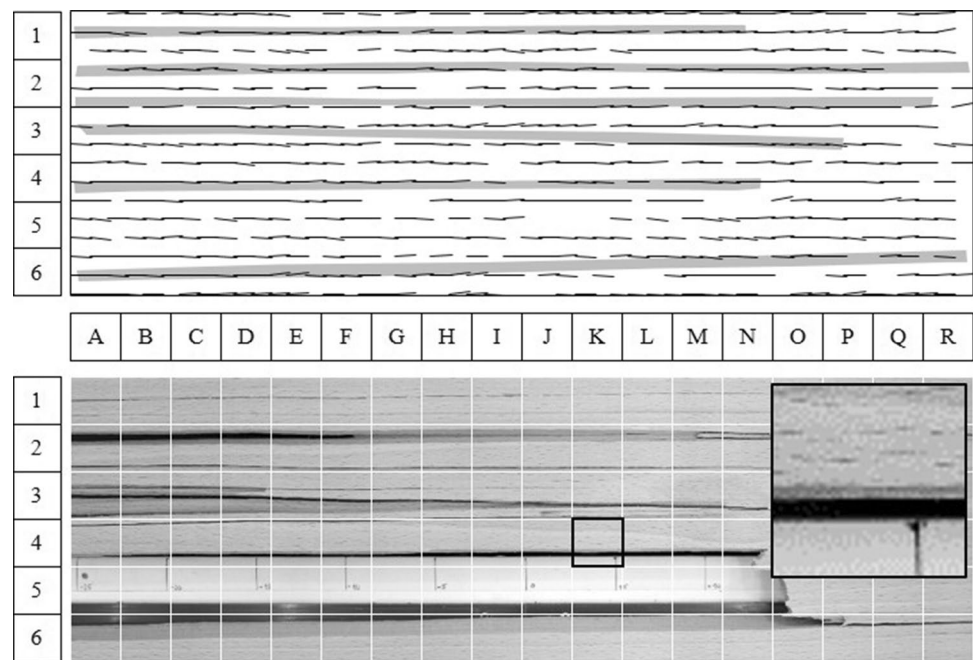


## 3.2 General evaluation of the method and discussion of possible improvements

Once again, the fact that commercially available equipment was used in all process steps has to be emphasized. Nevertheless, conclusive data could be generated that allowed for an already highly accurate prediction of the failure path in European beech timber boards showing various failure types.

However, especially in the edge regions of the images, the number of identified objects available for the estimation of fibre direction was considerably lower than in the centre parts, leading to limited information about the concerned areas. This has to be attributed to (1) the uneven illumination level, and (2) the image distortion related to the camera's lens not ideally suitable for this application.

Substantial improvement of the method regarding the quality of the estimates and the practical applicability could be achieved using a lens with a fixed focal width in order to reduce the distortion effects in the peripheral regions of the images. Furthermore, usage of a camera with a higher resolution would allow increasing the range of the images and/or their resolution.

Using a sensor with an optimised aspect ratio would allow taking account of the elongated shape of the area of interest and reducing the waste of pixels in non-board areas. Eventually, a line scan camera could meet the requirements regarding resolution, and, in combination with automated feeding, lead to a highly efficient process for the estimation of fibre direction of European beech wood.

Besides the mentioned improvements regarding the technical equipment, optimisation of the processing of data with respect to the discretisation of the wood volume, the calculation of representative values of the fibre direction and the visual and numerical description of the estimated field of fibre orientation is possible and advisable. However, once the orientation of fibres has been identified, advanced methods and algorithms currently implemented in other systems (e.g. employing the tracheid effect or thermal ellipsometry) may be adapted and also used for the presented method.

Due to the nature of the proposed method, only surfaces showing the medullary rays as a spindle pattern can be evaluated. This limits all investigations to the *LT*-plane, i.e. the wide face of flat sawn boards or the edge face of quarter-sawn boards, and planes with an inclination of approximately 45° to the *LT*-plane. However, experimental tensile tests of European beech timber boards have shown that the crucial fibre direction is predominantly determined by the medullary ray spindle pattern. Failure occurs in the *LR*-plane and, thus, an evaluation is just possible for the planes of interest.

## 3.3 Possible applications

The presented approach for the determination of fibre direction is expected to be not only suitable for European beech timber and its non-European relatives, such as American beech (*Fagus grandifolia* Ehrh.) and Japanese beech (*Fagus japonica* Maxim.), but also for other species with multi-row medullary rays. In Europe and North America, in particular oak (e.g. *Quercus rubra* L., *Quercus robur* L., and *Quercus alba* L.) has to be mentioned in this context.

Stress grading of the raw material is an important step in the production process of the established building products glued-laminated timber (GLT) and cross-laminated timber (CLT). For hardwoods, the fibre direction plays a key role in the estimation of strength and, thus, the presented method strongly contributes to the exploitation of their strength potential.

Regarding laminated veneer lumber (LVL), the issue of stress grading is of lower importance due to the high degree of homogenisation within this product. However, a non-contact method of potentially high feeding speed and accuracy could contribute to a better understanding and further improvement of the yield of this material being peeled and, thus, showing a perfect *LT*-plane surface.

Besides the building sector, hardwoods used for sports equipment and furniture must meet high requirements regarding strength and stiffness. The presented approach could help to push the limits and increase the reliability of highly stressed parts.

## 4 Conclusion

A non-contact method for the determination and documentation of fibre direction in European beech wood (F. *sylvatica* L.), based on the analysis of the spindles formed by the medullary rays, was presented and applied to specimens with five different types of grain pattern, subsequently subjected to tensile tests and evaluation of the resulting fracture pattern.

Fracture patterns resulting from tensile testing were used as reference, considered to reveal the true and *crucial fibre direction* of the timber boards. The estimated field of fibre direction of timber boards with a knot, local slope of grain, diving angle, general slope of grain, or splinter failure was found to be congruent with the reference fibre directions.

In contrast to other methods used for the determination of the fibre direction, for example based on radiographic systems or the tracheid effect, the presented approach directly uses a geometrical input without the need for an intermediate step based on another physical measure. Thus, the question is not how well the indicating parameter (e.g. the elliptical polarisation of originally linear polarised electromagnetic waves when using microwave scanning) is able to predict the target parameter (fibre direction), but how precise and accurate one is able to measure the indicator itself.

Improvements regarding the equipment and algorithms used for the detection and analysis of the medullary ray spindles will foreseeably lead to estimates of high quality and industrial usability. Currently used machines of different producers for the automated strength grading of wood, such as *Goldeneye 700* by *Microtec, WoodEye 5* by *WOODEYE AB*, and *CombiScan Evo* by *WEINIG*, are already equipped with one or several cameras, operating at feeding speeds of up to 450 m per minute. Provided that (1) the resolution of the implemented cameras and (2) the computing power of the used devices is sufficient, these machines might be straight away used for the strength grading of European beech or other hardwood species with multi-row medullary rays applying the presented method.

## References

Aicher S, Höfflin L, Behrens W (2001) A study on tension strength of finger joints in beech wood laminations. Otto Graf J 12:169–186

Ashby MF et al (1985) The fracture and toughness of woods. In: Proceedings of the Royal Society of London. Series A, Mathematical and Physical Sciences, pp 261–280

Baradit E, Aedo R, Correa J (2006) Knots detection in wood using microwaves. Wood Sci Technol 40(2):.118–123

Belkacemi M et al. (2016) Wood fiber orientation assessment based on punctual laser beam excitation: a preliminary study. In: Proceedings of the 2016 International Conference on Quantitative InfraRed Thermography (July)

Blaß HJ et al (2005) Biegefestigkeit von Brettschichtholz aus Buche (Bending strength of glued laminated timber made from beech) (In German). In: Karlsruher Berichte zum Ingenieurholzbau—Volume 1. Universitätsverlag Karlsruhe, Karlsruhe

Brännström M, Manninen J, Oja J (2008) Predicting the strength of sawn wood by tracheid laser scattering. BioResources 3(2):437–451

Briggert A, Olsson A, Oscarsson J (2016) Three-dimensional modelling of knots and pith location in Norway spruce boards using tracheid-effect scanning. Eur J Wood Prod 74(5):725–739

Clerc G, Volkmer T (2017) Brettschichtholz aus Laubholz - Technische Grundlagen zur Marktimplementierung als Bauprodukt in der Schweiz (Glued laminated timber made from hardwoods - Technical bases for the market implementation as a building product in Switzerland) (In German). Technical report of module 3, Biel, Switzerland

Cramer SM, McDonald KA (1989) Predicting lumber tensile stiffness and strength with local grain angle measurements and failure analysis. Wood Fiber Sci 21(1):393–410

Daval V, Pot G, Belkacemi M, Meriaudeau F, Collet R (2015) Automatic measurement of wood fiber orientation and knot detection using an optical system based on heating conduction. Opt Express 23(26):33529–33539

Denzler JK, Weidenhiller A (2015) Microwave scanning as an additional grading principle for sawn timber. Eur J Wood Prod 73(4):423–431

DIN 4074–5 (2008) Strength grading of wood—Part 5: sawn hard wood (in German). DIN German Institute for Standardization

Ehrhart T, Fink G, Steiger R, Frangu A (2016a) Experimental investigation of tensile strength and stiffness indicators regarding European beech timber. In: Proceedings of WCTE 2016, Vienna, Austria

Ehrhart T, Fink G, Steiger R, Frangi A (2016b) Strength grading of European beech lamellas for the production of GLT and CLT. In: Proceedings of INTER—Meeting Forty-Nine, Graz, Austria, pp 29–43

EN 1310 (1997) Round and sawn timber—method of measurement of features. CEN European Committee for Standardization

EN 408 (2012) Timber structures—structural timber and glued laminated timber—determination of some phyiscal and mechanical properties. CEN European Committee for Standardization

Federal Office for the Environment FOEN (2014) Swiss Statistical Yearbook of Forestry [Jahrbuch Wald und Holz—Annuaire La forêt et le bois]. UZ Nr. 1420, FOEN, Bern (in German and French)

Foley C (2001) A three-dimensional paradigm of fiber orientation in timber. Wood Sci Technol 35(5):453–465

Frühmann K, Burgert I, Stanzl-Tschegg SE, Tschegg EK (2003) Mode I fracture behaviour on the growth ring scale and cellular level of spruce (*Picea abies* [L.] Karst.) and beech (*Fagus sylvatica* L.) loaded in the TR crack propagation system. Holzforschung 57(6):653–660

Frühwald K (2004) Laubholz im Bauwesen und seine Festigkeitssortierung (Strength grading of hardwoods for the building sector) (In German). In: VI. Sympozium DREVO V STAVEBNYCH KONSTRUKCIACH, Kocovce, Slovakia, pp 105–118

Frühwald K, Schickhofer G (2005) Strength grading of hardwoods. In: Proceedings of the 14th international symposium on nondestructive testing of wood, Hanover, Germany

Glos P, Denzler JK (2004) Strength and stiffness behaviour of beech laminations for high strength glulam. In: Görlacher R (ed) CIB—meeting thirty-seven. Edinburgh, Scotland, p CIB-W18/37-6-3

Krapez J-C, Gardette G, Balageas DL (1996) Thermal ellipsometry in steady-state and by lock-in thermography: application to anisotropic materials characterization. In: Proceedings of quantitative infrared thermography QIRT '96 Eurotherm Seminar 50, pp. 257–262

Lukacevic M, Füssl J (2014) Numerical simulation tool for wooden boards with a physically based approach to identify structural failure. Eur J Wood Prod 72(4):497–508

Matthews PC, Beech BH (1976) US Patent 3,976,384: method and apparatus for detecting timber defects

Matthews PC, Soest JF (1986) US Patent 4,606,64: method for determining localized fiber angle in a three dimensional fibrous material

Metcalfe L, Dashner B (2002) US Patent 2002/0025061A1: high speed and reliable determination of lumber quality using grain influenced distortion effects

Norimoto M, Yamada T (1972) The dielectric properties of wood VI: on the dielectric properties of the chemical constituents of wood

and the dielectric anisotropy of wood. Wood Res Bull Wood Res Inst Kyoto Univ 52:31–43

Norton JAP, McLaughlan TA, Kusec DJ (1974) US Patent 3,805,156: wood slope of grain indicator

Nyström J (2003) Automatic measurement of fiber orientation in softwoods by using the tracheid effect. Comput Electron Agric 41(1–3):91–99

Olsson A, Oscarsson J (2017) Strength grading based on high resolution laser scanning and dynamic exication: a full scale investigation of performance. Eur J Wood Prod 75(1):17–31

Olsson A, Oscarsson J, Serrano E, Källsner B, Johansson M, Enquist B (2013) Prediction of timber bending strength and in-member cross-sectional stiffness variation on the basis of local wood fibre orientation. Eur J Wood Prod 71(3):319–333

Sarén MP, Serimaa R, Tolonen Y (2006) Determination of fiber orientation in Norway spruce using X-ray diffraction and laser scattering. Eur J Wood Prod 64(3):183–188

Sauter UH, Breinig L (2016) European Hardwoods for the Building Sector Reality of today—possibilities for tomorrow: WP 1: Hardwood resources in Europe Standing stock and resource forecasts. Workshop Garmisch-Partenkirchen

Schlotzhauer P et al. (2016) Machine grain angle determination on spruce, beech, and oak lumber for construction use. In: Proceedings of WCTE 2016, Vienna, Austria

Simonaho SP, Palviainen J, Tolonen Y, Silvennoinen R (2004) Determination of wood grain direction from laser light scattering pattern. Opt Lasers Eng 41(1):.95–103

Soest JF (1997) US Patent 5,703,960: lumber defect scanning including multi-dimensional pattern recognition

Steele PH, Neal SC, McDonald SM (1991) The slope-of-grain indicator for defect detection in unplaned hardwood lumber. For Prod J 41(1):15–20

Viguier J, Jehl A, Collet R, Bleron L, Meriaudeau F (2015) Improving strength grading of timber by grain angle measurement and mechanical modeling. Wood Mater Sci Eng 10(1):145–156

Viguier J, Bourreau D, Bocquet J-F, Pot G, Bleron L, Lanvin J-D (2017) Modelling mechanical properties of spruce and Douglas fir timber by means of X-ray and grain angle measurements for strength grading purpose. Eur J Wood Prod 75(4):527–541